



HAL
open science

A posteriori error estimates for the $DD+L^2$ jumps method on the Neutron Diffusion equations

Patrick Ciarlet, Minh-Hieu Do, Mario Gervais, François Madiot

► To cite this version:

Patrick Ciarlet, Minh-Hieu Do, Mario Gervais, François Madiot. A posteriori error estimates for the $DD+L^2$ jumps method on the Neutron Diffusion equations. 2024. cea-04714003

HAL Id: cea-04714003

<https://cea.hal.science/cea-04714003v1>

Preprint submitted on 30 Sep 2024

HAL is a multi-disciplinary open access archive for the deposit and dissemination of scientific research documents, whether they are published or not. The documents may come from teaching and research institutions in France or abroad, or from public or private research centers.

L'archive ouverte pluridisciplinaire **HAL**, est destinée au dépôt et à la diffusion de documents scientifiques de niveau recherche, publiés ou non, émanant des établissements d'enseignement et de recherche français ou étrangers, des laboratoires publics ou privés.

A posteriori error estimates for the DD+ L^2 jumps method on the Neutron Diffusion equations

Patrick Ciarlet¹, Minh Hieu Do², Mario Gervais², and François Madiot²

¹POEMS, CNRS, INRIA, ENSTA Paris, Institut Polytechnique de Paris, 91120 Palaiseau, France.

²Université Paris-Saclay, CEA, Service d'Études des Réacteurs et de Mathématiques Appliquées, 91191, Gif-sur-Yvette, France.

September 30, 2024

Abstract

We analyse *a posteriori* error estimates for the discretization of the neutron diffusion equations with a Domain Decomposition Method, the so-called DD+ L^2 jumps method. We provide guaranteed and locally efficient estimators on a base block equation, the one-group neutron diffusion equation. Classically, one introduces a Lagrange multiplier to account for the jumps on the interface. This Lagrange multiplier is used for the reconstruction of the physical variables. Remarkably, no reconstruction of the Lagrange multiplier is needed to achieve the optimal *a posteriori* estimates.

1 Introduction

The diffusion equation can model different physical phenomena, for instance Darcy's law, Fick's law or the neutron diffusion. Among models that are used in the nuclear industry, the multigroup neutron diffusion equation plays a central role [9]. The base block is the one-group neutron diffusion equation. In [8, 7], the first author and co-authors carried out the numerical analysis of this one-group neutron diffusion equation with a source term, discretized with mixed finite elements. The analysis included in particular the case of low-regularity solutions. *A priori estimates* were derived in the process. *A posteriori estimates* have been introduced more recently by the first and last co-authors for the mono-domain formulation of the base block equation[6]. A natural question is then

the extension of the *a posteriori* analysis to the Domain Decomposition+ L^2 -jumps method (or DD+ L^2 -jumps method) [8], to further optimize the cost of the numerical method. This is the main topic we address in this paper.

A *a posteriori* analysis for mixed finite elements has been extensively studied, see [4, 14, 15, 21] and references therein for the Poisson equation, [23, 22] for the diffusion-reaction equation (one-group neutron diffusion equation), and [20] for the convection-diffusion-reaction equation.

Nuclear reactor cores often have a Cartesian geometry. Indeed, in the models, the base brick, which is called a cell, is a rectangular cuboid of \mathbb{R}^3 . The global layout is a set of cells that are distributed on a 3D grid, so that the global domain of the reactor core is represented by a rectangular cuboid of \mathbb{R}^3 . Each cell can be made of fuel, absorbing or reflector material. To account for the different materials, the coefficients in the models are *piecewise polynomials* (possibly piecewise constant) with respect to the position, ie. their restriction to each cell is a polynomial [9, 12, 13].

The outline is as follows.

In Sections 2 and 3, we introduce some notations and our model problem. Then in Section 4, we recall how it can be solved in a mixed setting. To that aim, we build the standard equivalent variational formulation, and provide the existing *a priori* numerical analysis results that allow one to compare the discrete solution to the exact one. For the discretization, we choose the well-known Raviart-Thomas-Nédélec finite element RTN_k , where $k \geq 0$ denotes the order. In Section 5, we introduce the Domain Decomposition+ L^2 -jumps method.

In Section 6, we propose the *a posteriori* analysis of the model. We begin with the reconstruction of the solution, which can be devised in at least two ways: a post-processing or an averaging approach. In Section 7, we propose a numerical illustration of adaptive mesh refinement. For that, we focus on a specific discretization, based on Cartesian meshes. This kind of discretization is of particular importance for nuclear core simulations.

2 Notations

We choose the same notations as in [8, 7]. Throughout the paper, C is used to denote a generic positive constant which is independent of the mesh size, the mesh and the quantities/fields of interest. We also use the shorthand notation $A \lesssim B$ for the inequality $A \leq CB$, where A and B are two scalar quantities, and C is a generic constant.

Vector-valued (resp. tensor-valued) function spaces are written in boldface characters (resp. blackboard characters); for the latter, the index *sym* indicates symmetric fields. Given an open set $\mathcal{O} \subset \mathbb{R}^d$, $d = 1, 2, 3$, we use the notation $(\cdot, \cdot)_{0, \mathcal{O}}$ (respectively $\|\cdot\|_{0, \mathcal{O}}$) for the $L^2(\mathcal{O})$ and $\mathbf{L}^2(\mathcal{O}) = (L^2(\mathcal{O}))^d$ inner products (resp. norms). More generally, $(\cdot, \cdot)_{s, \mathcal{O}}$ and $\|\cdot\|_{s, \mathcal{O}}$ (respectively $|\cdot|_{s, \mathcal{O}}$) denote the inner product and norm (resp. semi-norm) of the Sobolev spaces $H^s(\mathcal{O})$ and $\mathbf{H}^s(\mathcal{O}) = (H^s(\mathcal{O}))^d$ for $s \in \mathbb{R}$ (resp. for $s > 0$).

When the boundary $\partial\mathcal{O}$ is Lipschitz, $\mathbf{n} \in \mathbf{L}^\infty(\partial\mathcal{O})$ denotes the unit outward

normal vector field to $\partial\mathcal{O}$. Finally, it is assumed that the reader is familiar with vector-valued function spaces related to the diffusion equation, such as $\mathbf{H}(\text{div}; \mathcal{O})$, $\mathbf{H}_0(\text{div}; \mathcal{O})$ etc.

Specifically, we let Ω be a bounded, connected and open subset of \mathbb{R}^d for $d = 2, 3$, having a Lipschitz boundary which is piecewise smooth. We split Ω into N open disjoint parts $\{\Omega_i\}_{1 \leq i \leq N}$ with Lipschitz, piecewise smooth boundaries: $\bar{\Omega} = \cup_{1 \leq i \leq N} \bar{\Omega}_i$ and the set $\{\Omega_i\}_{1 \leq i \leq N}$ is called a partition of Ω . For a field v defined over Ω , we shall use the notations $v_i = v|_{\Omega_i}$, for $1 \leq i \leq N$.

Given a partition $\{\Omega_i\}_{1 \leq i \leq N}$ of Ω , we introduce a function space with piecewise regular elements:

$$\mathcal{P}W^{1,\infty}(\Omega) = \{\psi \in L^\infty(\Omega) \mid \psi_i \in W^{1,\infty}(\Omega_i), 1 \leq i \leq N\}.$$

To measure $\psi \in \mathcal{P}W^{1,\infty}(\Omega)$, we use the natural norm

$$\|\psi\|_{\mathcal{P}W^{1,\infty}(\Omega)} = \max_{i=1,N} \|\psi_i\|_{W^{1,\infty}(\Omega_i)}.$$

3 The model

Given a source term $S_f \in L^2(\Omega)$, we consider the following neutron diffusion equation, with vanishing Dirichlet boundary condition. In its primal form, it is written:

$$\begin{cases} \text{Find } \phi \in H_0^1(\Omega) \text{ such that} \\ -\text{div } \mathbb{D} \mathbf{grad} \phi + \Sigma_a \phi = S_f \text{ in } \Omega, \end{cases} \quad (3.1)$$

where ϕ , \mathbb{D} , and Σ_a denote respectively the neutron flux, the diffusion coefficient and the macroscopic absorption cross section. Finally, S_f denotes the fission source. When solving the neutron diffusion equation, \mathbb{D} is scalar-valued. We choose to consider more generally that \mathbb{D} is a (symmetric) tensor-valued coefficient. The coefficients defining Problem (3.1) satisfy the assumptions:

$$\begin{cases} (\mathbb{D}, \Sigma_a) \in \mathbb{L}_{sym}^\infty(\Omega) \times L^\infty(\Omega), \\ \exists D_*, D^* > 0, \forall \mathbf{z} \in \mathbb{R}^d, D_* |\mathbf{z}|^2 \leq (\mathbb{D} \mathbf{z}, \mathbf{z}) \leq D^* |\mathbf{z}|^2 \text{ a.e. in } \Omega, \\ \exists (\Sigma_a)_*, (\Sigma_a)^* > 0, 0 < (\Sigma_a)_* \leq \Sigma_a \leq (\Sigma_a)^* \text{ a.e. in } \Omega. \end{cases} \quad (3.2)$$

Classically, Problem (3.1) is equivalent to the following variational formulation:

$$\begin{cases} \text{Find } \phi \in H_0^1(\Omega) \text{ such that} \\ \forall \psi \in H_0^1(\Omega), (\mathbb{D} \mathbf{grad} \phi, \mathbf{grad} \psi)_{0,\Omega} + (\Sigma_a \phi, \psi)_{0,\Omega} = (S_f, \psi)_{0,\Omega}. \end{cases} \quad (3.3)$$

Under the assumptions (3.2) on the coefficients, the primal problem (3.1) is well-posed, in the sense that for all $S_f \in L^2(\Omega)$, there exists one and only one solution $\phi \in H_0^1(\Omega)$ that solves (3.1), with the bound $\|\phi\|_{1,\Omega} \lesssim \|S_f\|_{0,\Omega}$. Provided that the coefficient \mathbb{D} is piecewise smooth, the solution has extra smoothness (see eg. Proposition 1 in [8]).

Instead of imposing a Dirichlet boundary condition on $\partial\Omega$, one can consider a Neumann or Fourier boundary condition $\mu_F \phi + (\mathbb{D} \mathbf{grad} \phi) \cdot \mathbf{n} = 0$, with

$\mu_F \geq 0$. All results are similar. Throughout the paper, we add remarks on the extension in the situation where $\Sigma_a \geq 0$ may vanish. In particular, the *a posteriori* analysis we propose covers both the pure diffusion case ($\Sigma_a = 0$), and the diffusion-reaction case ($(\Sigma_a)_* > 0$).

4 Variational formulation and discretization in the mono-domain case

Let us introduce the function spaces:

$$\begin{aligned} V &= H_0^1(\Omega); \\ \mathcal{H} &= \{ \xi = (\mathbf{q}, \psi) \in \mathbf{L}^2(\Omega) \times L^2(\Omega) \}, \|\xi\|_{\mathcal{H}} = (\|\mathbf{q}\|_{0,\Omega}^2 + \|\psi\|_{0,\Omega}^2)^{1/2}; \\ \mathcal{X} &= \{ \xi = (\mathbf{q}, \psi) \in \mathbf{H}(\text{div}, \Omega) \times L^2(\Omega) \}, \|\xi\|_{\mathcal{X}} = \left(\|\mathbf{q}\|_{\mathbf{H}(\text{div}, \Omega)}^2 + \|\psi\|_{0,\Omega}^2 \right)^{1/2}. \end{aligned}$$

From now on, we use the notations: $\zeta = (\mathbf{p}, \phi)$ and $\xi = (\mathbf{q}, \psi)$.

4.1 Mixed variational formulation

The solution ϕ to (3.1) belongs to $H^1(\Omega)$, so if one lets $\mathbf{p} = -\mathbb{D} \mathbf{grad} \phi \in \mathbf{L}^2(\Omega)$, the neutron diffusion problem may be written as:

$$\begin{cases} \text{Find } (\mathbf{p}, \phi) \in \mathbf{H}(\text{div}, \Omega) \times H_0^1(\Omega) \text{ such that} \\ -\mathbb{D}^{-1} \mathbf{p} - \mathbf{grad} \phi = 0 \text{ in } \Omega, \\ \text{div } \mathbf{p} + \Sigma_a \phi = S_f \text{ in } \Omega. \end{cases} \quad (4.1)$$

Solving the mixed problem (4.1) is equivalent to solving (3.1).

Proposition 4.1. *Let \mathbb{D}, Σ_a satisfy (3.2). The solution $(\mathbf{p}, \phi) \in \mathbf{H}(\text{div}, \Omega) \times H_0^1(\Omega)$ to (4.1) is such that ϕ is a solution to (3.1) with the same data. Conversely, the solution $\phi \in H_0^1(\Omega)$ to (3.1) is such that $(-\mathbb{D} \mathbf{grad} \phi, \phi) \in \mathbf{H}(\text{div}, \Omega) \times H_0^1(\Omega)$ is a solution to (4.1) with the same data.*

To obtain the variational formulation for the mixed problem (4.1), let $\mathbf{q} \in \mathbf{H}(\text{div}, \Omega)$ and $\psi \in L^2(\Omega)$, multiply the first equation of (4.1) by \mathbf{q} , the second equation of (4.1) by $\psi \in L^2(\Omega)$, and integrate over Ω . Adding up the contributions, one finds that:

$$-(\mathbb{D}^{-1} \mathbf{p}, \mathbf{q})_{0,\Omega} - (\mathbf{grad} \phi, \mathbf{q})_{0,\Omega} + (\psi, \text{div } \mathbf{p})_{0,\Omega} + (\Sigma_a \phi, \psi)_{0,\Omega} = (S_f, \psi)_{0,\Omega}. \quad (4.2)$$

One may integrate by parts the second term in the left-hand side, which yields: $-(\mathbf{grad} \phi, \mathbf{q})_{0,\Omega} = (\phi, \text{div } \mathbf{q})_{0,\Omega}$. We conclude that the solution to (4.1) also solves:

$$\begin{cases} \text{Find } (\mathbf{p}, \phi) \in \mathcal{X} \text{ such that for all } (\mathbf{q}, \psi) \in \mathcal{X}, \\ -(\mathbb{D}^{-1} \mathbf{p}, \mathbf{q})_{0,\Omega} + (\phi, \text{div } \mathbf{q})_{0,\Omega} + (\psi, \text{div } \mathbf{p})_{0,\Omega} + (\Sigma_a \phi, \psi)_{0,\Omega} = (S_f, \psi)_{0,\Omega}. \end{cases} \quad (4.3)$$

Because \mathbb{D} is a symmetric tensor field, the form

$$c : ((\mathbf{p}, \phi), (\mathbf{q}, \psi)) \mapsto -(\mathbb{D}^{-1} \mathbf{p}, \mathbf{q})_{0,\Omega} + (\phi, \operatorname{div} \mathbf{q})_{0,\Omega} + (\psi, \operatorname{div} \mathbf{p})_{0,\Omega} + (\Sigma_a \phi, \psi)_{0,\Omega} \quad (4.4)$$

is continuous, bilinear and symmetric on $\mathbf{H}(\operatorname{div}, \Omega) \times L^2(\Omega)$.

We may rewrite the variational formulation (4.3) as:

$$\begin{cases} \text{Find } (\mathbf{p}, \phi) \in \mathbf{H}(\operatorname{div}, \Omega) \times L^2(\Omega) \text{ such that} \\ \forall (\mathbf{q}, \psi) \in \mathbf{H}(\operatorname{div}, \Omega) \times L^2(\Omega), \quad c((\mathbf{p}, \phi), (\mathbf{q}, \psi)) = (S_f, \psi)_{0,\Omega}. \end{cases} \quad (4.5)$$

Proposition 4.2. *The solution $\zeta = (\mathbf{p}, \phi)$ to (4.5) satisfies (4.1). Hence, problems (4.5) and (4.1) are equivalent.*

One may prove that the mixed formulation (4.5) is well-posed, see Theorem 4.4 in [7]. As a matter of fact, the result is obtained by proving an inf-sup condition in $\mathcal{X} = \mathbf{H}(\operatorname{div}, \Omega) \times L^2(\Omega)$, which we recall here.

Theorem 4.1. *Let \mathbb{D} and Σ_a satisfy (3.2). Then, the bilinear symmetric form c fulfills an inf-sup condition.*

For further use, given $\zeta = (\mathbf{p}, \phi)$ and $\xi = (\mathbf{q}, \psi)$, we define two forms on $\mathbf{H}(\operatorname{div}, \Omega) \times L^2(\Omega)$

$$\begin{aligned} d_S(\zeta, \xi) &= (\mathbb{D}^{-1} \mathbf{p}, \mathbf{q})_{0,\Omega} + (\Sigma_a \phi, \psi)_{0,\Omega} \\ d(\zeta, \xi) &= d_S(\zeta, \xi) + (\psi, \operatorname{div} \mathbf{p})_{0,\Omega} - (\phi, \operatorname{div} \mathbf{q})_{0,\Omega} = c(\zeta, (-\mathbf{q}, \psi)). \end{aligned}$$

4.2 Discretization and *a priori* error analysis

We study conforming discretizations of (4.5). Let $(\mathcal{T}_h)_h$ be a family of meshes of Ω . We assume that there are made of (closed) polyhedra ($d = 3$) or polygons ($d = 2$), called *elements*, whose interior are mutually disjoint. The boundary of the elements are the union of (closed) *facets*: faces ($d = 3$) or edges ($d = 2$). The set of facets is denoted \mathcal{F}_h , and it is split as $\mathcal{F}_h = \mathcal{F}_h^\Omega \cup \mathcal{F}_h^{\partial\Omega}$, with $\mathcal{F}_h^{\partial\Omega} = \{F \in \mathcal{F}_h \mid F \subset \partial\Omega\}$ being the set of boundary facets, resp. $\mathcal{F}_h^\Omega = \{F \in \mathcal{F}_h \mid F \subset \Omega\}$ being the set of interior facets. An interior facet F is called an interface facet if $F \subset \Gamma$. For conforming discretization, those meshes are equal to meshes of $\bar{\Omega}$, that is tessellations of $\bar{\Omega}$ without hanging nodes (see eg. [5, Section 2.1]). They are made for instance of simplices, or of rectangles ($d = 2$), resp. cuboids ($d = 3$), indexed by a parameter h equal to the largest diameter of elements of a given mesh. We consider that elements are closed subsets of \mathbb{R}^d . We introduce discrete, finite-dimensional spaces $(\mathbf{Q}_h)_h, (L_h)_h$, indexed by h as follows:

$$\mathbf{Q}_h \subset \mathbf{H}(\operatorname{div}, \Omega), \text{ and } L_h \subset L^2(\Omega).$$

The conforming discretization of the variational formulation (4.5) is then:

$$\begin{cases} \text{Find } (\mathbf{p}_h, \phi_h) \in \mathbf{Q}_h \times L_h \text{ such that} \\ \forall (\mathbf{q}_h, \psi_h) \in \mathbf{Q}_h \times L_h, \quad c((\mathbf{p}_h, \phi_h), (\mathbf{q}_h, \psi_h)) = (S_f, \psi_h)_{0,\Omega}. \end{cases} \quad (4.6)$$

Following Corollary 26.15 in [11], we assume that $(\mathbf{Q}_h)_h$, resp. $(L_h)_h$ have the *approximability property* in the sense that

$$\begin{aligned} \forall \mathbf{q} \in \mathbf{H}(\operatorname{div}, \Omega), \quad \lim_{h \rightarrow 0} \left(\inf_{\mathbf{q}_h \in \mathbf{Q}_h} \|\mathbf{q} - \mathbf{q}_h\|_{\mathbf{H}(\operatorname{div}, \Omega)} \right) &= 0, \\ \forall \psi \in L^2(\Omega), \quad \lim_{h \rightarrow 0} \left(\inf_{\psi_h \in L_h} \|\psi - \psi_h\|_{0, \Omega} \right) &= 0. \end{aligned} \quad (4.7)$$

We also impose that the space L_h^0 of piecewise constant fields on the mesh is included in L_h , and that $\operatorname{div} \mathbf{Q}_h \subset L_h$. We finally define:

$$\mathcal{X}_h = \{ \xi_h = (\mathbf{q}_h, \psi_h) \in \mathbf{Q}_h \times L_h \}, \text{ endowed with } \|\cdot\|_{\mathcal{X}}.$$

Remark 4.1. *At some point, the discrete spaces are considered locally, i.e. restricted to one element of the mesh. So, one introduces the local spaces $\mathbf{Q}_h(K)$, $L_h(K)$ and $\mathcal{X}_h(K)$ for every $K \in \mathcal{T}_h$.*

Provided the above conditions are fulfilled, one may derive a uniform discrete inf-sup condition under the same assumptions as in Theorem 4.1 (cf. Theorem 4.5 in [7]).

Theorem 4.2. *Let $\mathbb{D} \in \mathcal{P}\mathbb{W}^{1, \infty}(\Omega)$, resp. $\Sigma_a \in \mathcal{P}W^{1, \infty}(\Omega)$, satisfy (3.2). Assume that $(\mathbf{Q}_h)_h$, $(L_h)_h$ fulfill (4.7), $L_h^0 \subset L_h$ and $\operatorname{div} \mathbf{Q}_h \subset L_h$ for all h . Then the bilinear form c fulfills a uniform discrete inf-sup condition in \mathcal{X}_h .*

The classical *a priori* error analysis follows. Let $\zeta_h = (\mathbf{p}_h, \phi_h)$ be the solution to (4.6).

Corollary 4.1. *Under the assumptions of Theorem 4.2, there holds:*

$$\exists C > 0, \quad \forall h, \quad \|\zeta - \zeta_h\|_{\mathcal{X}_h} \leq C \inf_{\xi_h \in \mathbf{x}_h} \|\zeta - \xi_h\|_{\mathcal{X}_h}. \quad (4.8)$$

Explicit *a priori* error estimates may be derived, see eg. [7].

In this paper, we focus on the Raviart-Thomas-Nédélec (RTN) Finite Element [19, 16].

For *simplicial meshes*, that is meshes made of simplices, the finite element spaces RTN_k can be described as follows, where $k \geq 0$ is the order of the discretization for the scalar fields of L_h , see eg. [3]. We denote by $\mathbb{P}_k(\mathcal{T}_h)$ the space of piecewise polynomials of maximal degree k on each simplex $K \in \mathcal{T}_h$.

The boundary of a simplex $K \in \mathcal{T}_h$ is made of the union of $(d-1)$ -simplices, the facets $(F_e^K)_{1 \leq e \leq d+1}$. We let $\mathbb{P}_k(K)$ be the space of polynomials of maximal degree k on K , resp. $\mathbb{P}_k(F_e^K)$ the space of polynomials of maximal degree k on F_e^K . The definition is

$$\operatorname{RTN}_k(K) = \{ \mathbf{q} \in \mathbf{L}^2(K) \mid \exists \mathbf{a} \in (\mathbb{P}_k(K))^d, \exists b \in \mathbb{P}_k(K), \forall \mathbf{x} \in K, \mathbf{q}(\mathbf{x}) = \mathbf{a} + b\mathbf{x} \}.$$

Observe that for all $\mathbf{q} \in \operatorname{RTN}_k(K)$, for all $e \in \{1, \dots, d+1\}$, $(\mathbf{q} \cdot \mathbf{n})|_{F_e^K} \in \mathbb{P}_k(F_e^K)$. The definitions of the finite element spaces RTN_k are then

$$\begin{aligned} \mathbf{Q}_h &= \{ \mathbf{q}_h \in \mathbf{H}(\operatorname{div}, \Omega) \mid \forall K \in \mathcal{T}_h, \mathbf{q}_h|_K \in \operatorname{RTN}_k(K) \}, \\ L_h &= \{ \psi_h \in L^2(\Omega) \mid \forall K \in \mathcal{T}_h, \psi_h|_K \in \mathbb{P}_k(K) \}. \end{aligned}$$

For *rectangular or Cartesian meshes*, a description of the Raviart-Thomas-Nédélec (RTN) finite element spaces can be found for instance in Section 4.2 of [13].

5 The DD+ L^2 -jumps method

In this section, we present a domain decomposition method introduced in [8], namely the DD+ L^2 -jumps method.

To this aim, let us consider a partition $\{\Omega_{i^*}^*\}_{1 \leq i^* \leq N^*}$ of Ω which is independent of the physical partition $\{\Omega_i\}_{1 \leq i \leq N}$ introduced in Section 2. For a field v defined over Ω , we shall use the notation $v_{i^*} = v|_{\Omega_{i^*}^*}$, for $1 \leq i^* \leq N^*$. We denote by $\Gamma_{i^*j^*}$ the interface between two subdomains $\Omega_{i^*}^*$ and $\Omega_{j^*}^*$ for $i^* \neq j^*$: if $\dim_H(\partial\Omega_{i^*}^* \cap \partial\Omega_{j^*}^*) = d-1$, then $\Gamma_{i^*j^*} = \text{int}(\partial\Omega_{i^*}^* \cap \partial\Omega_{j^*}^*)$; otherwise, $\Gamma_{i^*j^*} = \emptyset$. By construction, $\Gamma_{i^*j^*} = \Gamma_{j^*i^*}$. We define the interface Γ by

$$\Gamma = \cup_{i^*=1}^{N^*} \cup_{j^*=i^*+1}^{N^*} \overline{\Gamma_{i^*j^*}}.$$

We also introduce the function spaces¹

$$\begin{aligned} PH_0^1(\Omega) &= \{\psi \in L^2(\Omega) \mid \psi_{i^*} \in H^1(\Omega_{i^*}^*), \psi|_{\partial\Omega_{i^*}^* \setminus \Gamma} = 0, 1 \leq i^* \leq N^*\}, \\ \mathbf{PH}(\text{div}, \Omega) &= \{\mathbf{q} \in L^2(\Omega) \mid \mathbf{q}_{i^*} \in \mathbf{H}(\text{div}, \Omega_{i^*}^*), 1 \leq i^* \leq N^*\}, \\ M &= \{m = (m_{i^*j^*})_{i^* < j^*} \in \prod_{i^* < j^*} L^2(\Gamma_{i^*j^*})\}, \\ \mathbf{Q}^* &= \{\mathbf{q} \in \mathbf{PH}(\text{div}, \Omega) \mid [\mathbf{q} \cdot \mathbf{n}] \in M\}, \\ \mathbb{W} &= \mathbf{Q}^* \times L^2(\Omega) \times M, \end{aligned}$$

where $[\mathbf{q} \cdot \mathbf{n}]$ stands for the global jump of the normal component on the interface $\Gamma_{i^*j^*} \neq \emptyset$ and is defined by

$$[\mathbf{q} \cdot \mathbf{n}]|_{\Gamma_{i^*j^*}} = \mathbf{q}_{i^*} \cdot \mathbf{n}_{i^*} + \mathbf{q}_{j^*} \cdot \mathbf{n}_{j^*}, \text{ for } 1 \leq i^* < j^* \leq N^*.$$

These spaces are endowed with their natural norm, eg.

$$\|m\|_M = \left(\sum_{1 \leq i^* < j^* \leq N^*} \|m_{i^*j^*}\|_{0, \Gamma_{i^*j^*}}^2 \right)^{1/2}.$$

We consider the following problem in the multi-domain case:

$$\left\{ \begin{array}{l} \text{Find } (\mathbf{p}, \phi, \ell) \in \mathbf{Q}^* \times PH_0^1(\Omega) \times M \text{ such that} \\ -\mathbb{D}_{i^*}^{-1} \mathbf{p}_{i^*} - \mathbf{grad} \phi_{i^*} = 0 \quad \text{in } \Omega_{i^*}^*, \quad \text{for } 1 \leq i^* \leq N^*, \\ \text{div } \mathbf{p}_{i^*} + \sum_{a, i^*} \phi_{i^*} = S_{f, i^*} \quad \text{in } \Omega_{i^*}^*, \quad \text{for } 1 \leq i^* \leq N^*, \\ \phi_{i^*} = \ell \quad \text{on } \Omega_{i^*}^* \cap \Gamma, \quad \text{for } 1 \leq i^* \leq N^*, \\ [\mathbf{p} \cdot \mathbf{n}] = 0 \quad \text{on } \Gamma. \end{array} \right. \quad (5.1)$$

¹By a slight abuse of notation, we identify M with $\prod_{i^* < j^*} L^2(\Gamma_{i^*j^*})$, and we consider that any tuple of M also belongs to $L^2(\Gamma)$, and vice versa. In particular, one can consider the restriction to one or several interfaces. Similarly for $PH_0^1(\Omega)$, $\mathbf{PH}(\text{div}, \Omega)$, and their elements.

The equivalent variational formulation writes

$$\begin{cases} \text{Find } \mathbf{u} = (\mathbf{p}, \phi, \ell) \in \mathbb{W} \text{ such that for all } \mathbf{w} = (\mathbf{q}, \psi, m) \in \mathbb{W}, \\ c_{DD}(\mathbf{u}, \mathbf{w}) = f(\mathbf{w}). \end{cases} \quad (5.2)$$

Extending the definition (4.4) of the bilinear form c to piecewise smooth fields by replacing \int_{Ω} by $\sum_{i^*=1}^{N^*} \int_{\Omega_{i^*}}$, one uses the forms

$$c_{DD}(\mathbf{u}, \mathbf{w}) = c((\mathbf{p}, \phi), (\mathbf{q}, \psi)) + \int_{\Gamma} [\mathbf{p} \cdot \mathbf{n}]m - \int_{\Gamma} [\mathbf{q} \cdot \mathbf{n}]\ell, \quad \text{and } f(\mathbf{w}) = (S_f, \psi)_{0, \Omega}.$$

In addition to the physical variables \mathbf{p} and ϕ , the field ℓ can be seen as a Lagrange multiplier. Let us recall the equivalence between the multi-domain Problem (5.1) and the mono-domain Problem (4.1).

Proposition 5.1 (Theorem 1 of [8]). *The triple $(\mathbf{p}, \phi, \ell) \in \mathbb{W}$ solves (5.2) if, and only if, ϕ solves (3.3) with the same data.*

Hence, combining Propositions 4.1 and 5.1, we find that Problems (4.1) and (5.1) are equivalent.

Remark 5.1. *The form c_{DD} is used for the a priori studies, while the forms c , d and d_S are used for the a posteriori estimates.*

We introduce discrete, finite-dimensional, spaces indexed by h as follows: $\mathbf{Q}_{i^*, h} \subset \mathbf{H}(\text{div}, \Omega_{i^*}^*)$ and $L_{i^*, h} \subset L^2(\Omega_{i^*}^*)$, for $1 \leq i^* \leq N^*$. We impose the following requirements for all $1 \leq i^* \leq N^*$:

- $\mathbf{q}_{i^*, h} \cdot \mathbf{n} \in L^2(\partial\Omega_{i^*}^*)$ for all $h > 0$, for all $\mathbf{q}_{i^*, h} \in \mathbf{Q}_{i^*, h}$;
- $\text{div } \mathbf{Q}_{i^*, h} \subset L_{i^*, h}$ for all $h > 0$;
- $(\mathbf{Q}_{i^*, h})_h$ and $(L_{i^*, h})_h$ satisfy the approximability property (4.7) in $\Omega_{i^*}^*$.

We observe that, to build conforming discretizations in $\mathbf{PH}(\text{div}, \Omega)$, one uses meshes that are *conforming* with respect to the partition $\{\Omega_{i^*}^*\}_{1 \leq i^* \leq N^*}$. One first defines, for $1 \leq i^* \leq N^*$, families of *conforming* meshes $(\mathcal{T}_{h, i^*})_h$ of $\Omega_{i^*}^*$. Then, the meshes $(\mathcal{T}_h)_h$ are built by aggregating for given h the meshes $(\mathcal{T}_{h, i^*})_{1 \leq i^* \leq N^*}$. If $\Omega_{i^*}^*$ and $\Omega_{j^*}^*$ share a common (non-empty) interface $\Gamma_{i^* j^*}$, the meshes \mathcal{T}_{h, i^*} and \mathcal{T}_{h, j^*} are said to be *matching* if their restriction to $\Gamma_{i^* j^*}$ coincide. Otherwise, they are *non-matching*. As soon as there is a pair of non-matching meshes, the mesh \mathcal{T}_h is not *conforming*: we call this situation the *non-matching case*. On the contrary, when all pairs of meshes are matching, \mathcal{T}_h itself is a *conforming* mesh: we call this situation the *matching case*.

Introducing the discrete space of Lagrange multipliers $M_h \subset M$, we then set

$$\mathbf{Q}_h^* = \prod_{i^*=1}^{N^*} \mathbf{Q}_{i^*, h}, \quad L_h^* = \prod_{i^*=1}^{N^*} L_{i^*, h}, \quad \mathbb{W}_h = \mathbf{Q}_h^* \times L_h^* \times M_h,$$

We assume that the space of piecewise constant fields is included in M_h . The discrete variational formulation associated to (5.2) writes

$$\begin{cases} \text{Find } \mathbf{u}_h = (\mathbf{p}_h, \phi_h, \ell_h) \in \mathbb{W}_h \text{ such that for all } \mathbf{w}_h = (\mathbf{q}_h, \psi_h, m_h) \in \mathbb{W}_h, \\ c_{DD}(\mathbf{u}_h, \mathbf{w}_h) = f(\mathbf{w}_h). \end{cases} \quad (5.3)$$

Following [8, Section 5], we define the discrete L^2 -projection operators $(\Pi_{i^*})_{1 \leq i^* \leq N^*}$ from the spaces of normal traces

$$T_{i^*,h} = \{t_{i^*,h} \in L^2(\partial\Omega_{i^*}^* \cap \Gamma) \mid \exists \mathbf{q}_{i^*,h} \in \mathbf{Q}_{i^*,h}, t_{i^*,h} = \mathbf{q}_{i^*,h} \cdot \mathbf{n}_{i^*|_{\partial\Omega_{i^*}^* \cap \Gamma}}\},$$

for $1 \leq i^* \leq N^*$, to M_h ,² resp. the discrete L^2 -projection operators $(\pi_{i^*})_{1 \leq i^* \leq N^*}$ from M_h to $(T_{i^*,h})_{1 \leq i^* \leq N^*}$, which are defined by

$$\begin{aligned} \forall t_{i^*,h} \in T_{i^*,h}, \forall m_h \in M_h, \\ \begin{cases} \int_{\partial\Omega_{i^*}^* \cap \Gamma} (\Pi_{i^*} t_{i^*,h} - t_{i^*,h}) m_h = 0 \\ \int_{\partial\Omega_{i^*}^* \cap \Gamma} (\pi_{i^*} m_h - m_h) t_{i^*,h} = 0. \end{cases} \end{aligned}$$

Next, let $\mathbf{p}_h \in \mathbf{Q}_h^*$. We define the *discrete jump* of the normal component of \mathbf{p}_h on the interface $\Gamma_{i^*j^*}$ as $[\mathbf{p}_h \cdot \mathbf{n}]_{h,i^*j^*} := \Pi_{i^*}(\mathbf{p}_{i^*,h} \cdot \mathbf{n}_{i^*|_{\Gamma_{i^*j^*}}}) + \Pi_{j^*}(\mathbf{p}_{j^*,h} \cdot \mathbf{n}_{j^*|_{\Gamma_{i^*j^*}}})$.

Assumption 5.1. *We assume that there exists $\beta_h > 0$ such that for all $\mathbf{q}_h \in \mathbf{Q}_h^*$,*

$$\int_{\Gamma} [\mathbf{q}_h \cdot \mathbf{n}]_h [\mathbf{q}_h \cdot \mathbf{n}] \geq \beta_h \int_{\Gamma} [\mathbf{q}_h \cdot \mathbf{n}]^2, \quad (5.4)$$

and that there exists $\gamma_h > 0$ such that for all $m_h \in M_h$,

$$\sum_{i^*=1}^{N^*} \sum_{j^*=i^*+1}^{N^*} \int_{\Gamma_{i^*j^*}} ((\pi_{i^*} m_h)^2 + (\pi_{j^*} m_h)^2) \geq \gamma_h \|m_h\|_M^2. \quad (5.5)$$

We refer to [8, Section 5.2] for an extensive discussion on how to fulfill this assumption in practice. In particular (see §5.2.1 in [8]), the choice

$$M_h = \sum_{i^*=1}^{N^*} T_{i^*,h} \quad (5.6)$$

is a sufficient condition. It is proven in [8, Section 5.1] that, under Assumption 5.1:

- the discrete problem (5.3) is well-posed;
- the discrete solution fulfills $[\mathbf{p}_h \cdot \mathbf{n}] = 0$, so that $\mathbf{p}_h \in \mathbf{H}(\text{div}, \Omega)$.

²More precisely, from $T_{i^*,h}$ to $\{m_h \in M_h \mid \text{supp}(m_h) \subset \partial\Omega_{i^*}^* \cap \Gamma\}$.

6 *A posteriori* studies for the DD+ L^2 jumps method

To develop the study of *a posteriori* estimates, we use the so-called reconstruction of the discrete solution $\mathbf{u}_h = (\mathbf{p}_h, \phi_h, \ell_h) \in \mathbf{W}_h$. More precisely, we are interested in the reconstruction of the physical variables. Nevertheless, the Lagrange multiplier ℓ_h may play a role in the reconstruction. We denote by $\tilde{\zeta}_h = (\tilde{\mathbf{p}}_h, \tilde{\phi}_h)$ a reconstruction, and by $\eta := \eta(\tilde{\zeta}_h)$ an estimator. Classically, our aim is to obtain *reliable* and *efficient* estimators for the reconstructed error $\zeta - \tilde{\zeta}_h$, meaning that:

$$\begin{aligned} \|\zeta - \tilde{\zeta}_h\| &\leq \mathbf{C} \eta \quad (\text{reliability}) \\ \eta &\leq \mathbf{c} \|\zeta - \tilde{\zeta}_h\| \quad (\text{efficiency}) \end{aligned}$$

where \mathbf{C} and \mathbf{c} are generic constants, and $\|\cdot\|$ is some norm to measure the error. In what follows, we choose to look for $\tilde{\zeta}_h := \tilde{\zeta}_h(\mathbf{p}_h, \phi_h, \ell_h) \in \mathbf{H}(\text{div}, \Omega) \times V$. Since under Assumption 5.1, one has $\mathbf{p}_h \in \mathbf{H}(\text{div}, \Omega)$, one can set $\tilde{\mathbf{p}}_h = \mathbf{p}_h$. Finally, we will design $\tilde{\phi}_h$ as a function of (ϕ_h, ℓ_h) . To summarize, we will consider from this point on reconstructions like

$$\tilde{\zeta}_h = (\mathbf{p}_h, \tilde{\phi}_h(\phi_h, \ell_h)) \in \mathbf{H}(\text{div}, \Omega) \times V.$$

In Section 6.1, we recall some reconstruction approaches for RTN finite element spaces. Section 6.2 is devoted to the derivation of *a posteriori* estimates.

6.1 Reconstruction of the discrete solution

In this section, we investigate some approaches to devise a reconstruction of the discrete solution $(\mathbf{p}_h, \phi_h, \ell_h)$, here obtained with the DD+ L^2 jumps method on the RTN $_k$ finite element discretization, for $k \geq 0$. We first focus on the abstract theory (developed below for simplicial meshes), and then on practical implementation algorithms (illustrated below on Cartesian meshes). The reverse can be done without difficulty.

As mentioned above, we want to build a reconstruction $\tilde{\phi}_h$ that belongs to V . So, we let $\tilde{\mathcal{T}}_h$ be the mesh on which a V -conforming Lagrange Finite Element space $V_h^{k'}$ of order $k' \geq 0$ is defined, respectively $\tilde{\mathcal{V}}_h^{k'}$ be the set of nodes where the degrees of freedom of $V_h^{k'}$ are defined. And, for a node $a \in \tilde{\mathcal{V}}_h^{k'}$, we denote by \mathcal{T}_a the set of simplices $K \in \mathcal{T}_h$ such that $a \in K$ and by \mathcal{E}_a the set of interface facets of \mathcal{T}_h sharing a .

In the matching case, the definition of $V_h^{k'}$ is natural and hinges on the matching meshes. In the non-matching case, there is more freedom of choice to define such a space. A first idea is to construct a V -conforming mesh $\tilde{\mathcal{T}}_h$ such that $\tilde{\mathcal{T}}_h$ is a refinement of \mathcal{T}_h . An alternative is to construct a V -conforming mesh $\tilde{\mathcal{T}}_h$ such that \mathcal{T}_h is a refinement of $\tilde{\mathcal{T}}_h$. More generally, in both cases, we emphasize that it is possible to choose a mesh $\tilde{\mathcal{T}}_h$ which contains hanging nodes as long as the definition of the reconstruction operator ensures that its range is included in V .

6.1.1 Reconstruction theory for simplicial meshes

Let us consider the case of simplicial meshes.

We first extend the averaging operator defined in [6, Section 5.1.1.]. See [17] for the (original) Oswald interpolation operator and [20] for another modified version. We introduce the averaging operator of the neutron flux $\mathcal{I}_{av} : \mathbb{P}_k(\mathcal{T}_h) \rightarrow V_h^{k+1}$ such that

$$\forall \phi_h \in \mathbb{P}_k(\mathcal{T}_h), \forall a \in \tilde{\mathcal{V}}_h^{k+1}, \quad \mathcal{I}_{av}(\phi_h)(a) = \begin{cases} \frac{1}{|\mathcal{E}_a|} \sum_{E \in \mathcal{E}_a} \ell_{h|E}(a) & \text{if } a \in \text{int}(\Gamma), \\ \frac{1}{|\mathcal{T}_a|} \sum_{K \in \mathcal{T}_a} \phi_{h|K}(a) & \text{otherwise.} \end{cases}$$

The *average reconstruction* is

$$\tilde{\zeta}_{av,h} = (\mathbf{p}_h, \mathcal{I}_{av}(\phi_h)). \quad (6.1)$$

In order to recover the relation $\mathbf{p} = -\mathbb{D} \mathbf{grad} \phi$ at the discrete level, some post-processing techniques have been introduced for the mixed finite element method [20, 21]. We extend here the approach proposed in [1], valid for $k \geq 0$. The idea is to consider a hybrid formulation, where the constraint on the continuity of the normal trace of \mathbf{p}_h is relaxed. For $1 \leq i^* \leq N^*$, let $\mathcal{F}_h(\mathcal{T}_{h,i^*})$ be the set of facets associated to the mesh \mathcal{T}_{h,i^*} , respectively $\Gamma_{i^*}^F$ the union of interior facets of $\mathcal{F}_h(\mathcal{T}_{h,i^*})$, i.e. the union of the facets of $\mathcal{F}_h(\mathcal{T}_{h,i^*}) \cap \mathcal{F}_h^\Omega$. Let

$$\Lambda_h = \sum_{i^*=1}^{N^*} \Lambda_{h,i^*},$$

where, for $1 \leq i^* \leq N^*$,

$$\Lambda_{h,i^*} = \{ \mu_h \in L^2(\Gamma_{i^*}^F) \mid \exists \mathbf{q}_h \in \mathbf{Q}_{i^*,h} \text{ such that } \forall F \in \mathcal{F}_h(\mathcal{T}_{h,i^*}) \cap \mathcal{F}_h^\Omega, \mu_{h|F} = \mathbf{q}_h \cdot \mathbf{n}_{|F} \}$$

is the space of the Lagrange multipliers³ and let $\bar{\mathcal{X}}_h = \Pi_{K \in \mathcal{T}_h} \mathcal{X}_h(K)$ be the unconstrained approximation space with the RTN_k local finite element spaces. By definition, \mathcal{X}_h is a strict subset of $\bar{\mathcal{X}}_h$.

The hybrid formulation is:

$$\left\{ \begin{array}{l} \text{Find } ((\bar{\mathbf{p}}_h, \bar{\phi}_h), \bar{\lambda}_h) \in \bar{\mathcal{X}}_h \times \Lambda_h \text{ such that } \forall ((\mathbf{q}_h, \psi_h), \mu_h) \in \bar{\mathcal{X}}_h \times \Lambda_h, \\ c((\bar{\mathbf{p}}_h, \bar{\phi}_h), (\mathbf{q}_h, \psi_h)) - \sum_{F \in \mathcal{F}_h^\Omega} \int_F \bar{\lambda}_h[\mathbf{q}_h \cdot \mathbf{n}] + \sum_{F \in \mathcal{F}_h^\Omega} \int_F \mu_h[\bar{\mathbf{p}}_h \cdot \mathbf{n}] = (S_f, \psi_h)_{0,\Omega}. \end{array} \right. \quad (6.2)$$

³ In each $\Gamma_{i^*}^F$, there are facets that lie on the interface. So, regarding the definition of Λ_h on facets of a given interface, it is equal to the sum of the two normal trace spaces coming from both sides of the interface. If the meshes are matching, this sum coincides with either normal trace space. On the other hand, if the meshes are non-matching, one must explicitly build the sum.

We may reinterpret Problem (6.2) as the application of the DD+ L^2 jumps method where each $K \in \mathcal{T}_h$ is a subdomain and the discrete space of Lagrange multipliers is chosen as the sum of the discrete normal traces. According to [8, Section 5.2.1], Assumption 5.1 applies for Problem (6.2). So the discrete problem (6.2) is well-posed and the discrete solution fulfills $[\bar{\mathbf{p}}_h \cdot \mathbf{n}]|_F = 0$ for all $F \in \mathcal{F}_h^\Omega$: the latter is checked simply by taking the test-function $((0, 0), ([\bar{\mathbf{p}}_h \cdot \mathbf{n}]|_F)_{F \in \mathcal{F}_h^\Omega})$. Hence, we have that $\bar{\mathbf{p}}_h \in \mathbf{Q}_h^* \cap \mathbf{H}(\text{div}, \Omega)$. We infer that $(\bar{\zeta}_h, \bar{\lambda}_h|_\Gamma)$ is solution to Problem (5.3) with M_h chosen as in (5.6). The idea is to project the solution of the hybrid formulation (6.2) to an appropriate augmented space. The projection operator is defined similarly as in [6, Section 5.1.2]. For the sake of completeness, we recall here its definition, $\Pi_{\mathcal{M}_h} : \bar{\mathcal{X}}_h \times \Lambda_h \rightarrow \mathcal{M}_h$ the projection onto the appropriate augmented space \mathcal{M}_h such that, given $(\bar{\zeta}_h, \lambda_h) \in \bar{\mathcal{X}}_h \times \Lambda_h$ where $\bar{\zeta}_h = (\bar{\mathbf{p}}_h, \bar{\phi}_h)$, its projection $\hat{\phi}_h = \Pi_{\mathcal{M}_h}(\bar{\zeta}_h, \lambda_h)$ is governed by

$$\begin{aligned} \forall (\psi_h, \mu_h) \in L_h^* \times \Lambda_h, \\ (\Sigma_a \hat{\phi}_h, \psi_h)_{0,\Omega} + \sum_{F \in \mathcal{F}_h^\Omega} \int_F \hat{\phi}_h \mu_h = (\Sigma_a \bar{\phi}_h, \psi_h)_{0,\Omega} + \sum_{F \in \mathcal{F}_h^\Omega} \int_F \lambda_h \mu_h. \end{aligned}$$

We refer to [6, Section 5.1.2] for the definition of the space \mathcal{M}_h and to [6, Section 5.1.2] for the situation where $\Sigma_a \geq 0$ may vanish which remains valid here.

The RTN *post-processing* $\mathcal{I}_{\text{RTN}}^2 : \bar{\mathcal{X}}_h \times \Lambda_h \rightarrow V_h^{k+2}$ is defined here by,

$$\begin{aligned} \forall (\bar{\zeta}_h, \lambda_h) \in \bar{\mathcal{X}}_h \times \Lambda_h, \forall a \in \tilde{\mathcal{V}}_h^{k+2}, \\ \mathcal{I}_{\text{RTN}}^2(\bar{\zeta}_h, \lambda_h)(a) = \begin{cases} \frac{1}{|\mathcal{E}_a|} \sum_{E \in \mathcal{E}_a} \lambda_h|_E(a) & \text{if } a \in \text{int}(\Gamma), \\ \frac{1}{|\mathcal{T}_a|} \sum_{K \in \mathcal{T}_a} (\Pi_{\mathcal{M}_h}(\bar{\zeta}_h, \lambda_h))|_K(a) & \text{otherwise.} \end{cases} \end{aligned}$$

Finally, the *reconstruction* associated to the RTN post-processing is

$$\tilde{\zeta}_{\text{RTN},h} = (\mathbf{p}_h, \mathcal{I}_{\text{RTN}}^2(\bar{\zeta}_h, \lambda_h)). \quad (6.3)$$

Remark 6.1. *It is worth noticing that the possibility to enforce, for a reconstruction, the conservation of local averages by adding bubble functions is still valid [6, Section 5.1.3].*

6.1.2 Reconstruction algorithms for Cartesian meshes

Let us consider the case of Cartesian meshes. Below we focus on practical algorithms.⁴ In the reconstruction of the discrete solution of the DD+ L^2 -jumps method, it may be necessary to tackle non conformities at the interface.

⁴Observe that the abstract results presented in Section 6.1.1 can be extended to the case of rectangular or cuboid meshes [21].

We detail here a possible approach to define the reconstruction where the mesh may contain hanging nodes with structured, Cartesian meshes. Specifically, we consider next a two-dimensional domain divided into $N^* = 3$ subdomains. Starting from an $\text{RTN}_0 \times \mathbb{Q}^0 \times \mathbb{Q}^0$ finite element discretisation $(\mathbf{p}_h, \phi_h, \lambda_h)$, we propose an explicit V -conforming algorithm to build a reconstruction $\tilde{\phi}_h$ with \mathbb{Q}^1 finite elements.

We compute first an intermediate reconstruction $\phi_{h,\text{disc}} \in PH_0^1(\Omega)$ defined on the mesh \mathcal{T}_h (see Figure 1, left), using a reconstruction operator independently on each subdomain $\Omega_{i^*}^*$ for $1 \leq i^* \leq N^*$. Second, we create a mesh by projecting the nodes located at the non-conformities of the interface onto the mesh of the *neighbouring* subdomain. This defines a reconstruction mesh called $\tilde{\mathcal{T}}_h$ (see Figure 1, right). Using $\phi_{h,\text{disc}}$ and the discrete Lagrange multiplier ℓ_h , it is possible to devise a V -conforming reconstruction $\tilde{\phi}_h$ on $\tilde{\mathcal{T}}_h$. The method we detail here and use in Section 7 can be seen as an extension of the averaging method. It could be adapted without loss of genericity to any intermediate reconstruction $\phi_{h,\text{disc}}$.

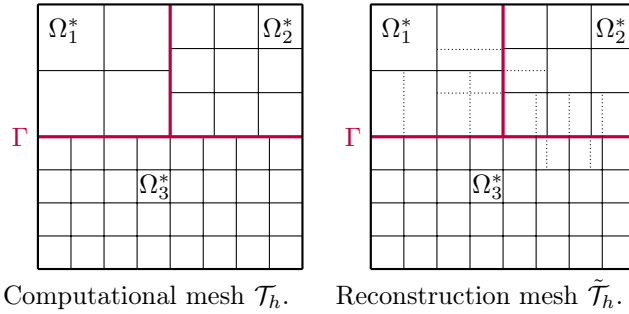


Figure 1: Computational mesh \mathcal{T}_h and reconstruction mesh $\tilde{\mathcal{T}}_h$.

For $1 \leq i^* \leq N^*$, let $\mathcal{V}_h(\mathcal{T}_{h,i^*})$ be the set of vertices associated to the \mathbb{Q}^1 Lagrange finite element space on the mesh \mathcal{T}_{h,i^*} . Then, $\mathcal{V}_{h,\text{disc}} = \cup_{i^*=1,N^*} \mathcal{V}_h(\mathcal{T}_{h,i^*})$ is the set of nodes associated to the degrees of freedom of a $PH_0^1(\Omega)$ -conforming space (see Figure 2 for the nodes).

The intermediate reconstruction $\phi_{h,\text{disc}}$ is built subdomain by subdomain, and characterized by

$$\text{for } 1 \leq i^* \leq N^*, \forall a \in \mathcal{V}_h(\mathcal{T}_{h,i^*}),$$

$$\phi_{h,\text{disc}}(a) = \begin{cases} \frac{1}{|\mathcal{E}_a|} \sum_{E \in \mathcal{E}_a} \ell_{h|E}(a) & \text{if } a \in \text{int}(\Gamma), \\ \frac{1}{|\mathcal{T}_a|} \sum_{K \in \mathcal{T}_a} \phi_{h|K}(a) & \text{otherwise.} \end{cases}$$

We observe that hanging nodes can create discontinuities at the interfaces, because it may occur that 5 or more degrees of freedom are computed in one element. We address this difficulty next. More precisely, for elements K that

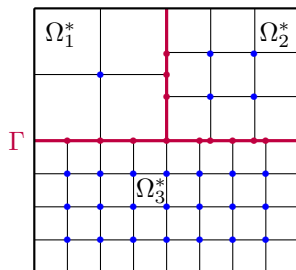


Figure 2: Available nodes for the intermediate reconstruction $\phi_{h,\text{disc}}$. Interface nodes are in purple, nodes in the subdomains are in blue.

intersect with the interface, if at least one facet does not coincide with an interior facet in \mathcal{F}_h^Ω , we build a Cartesian refinement of the cell K by taking into account all the interior facets included in ∂K . The new mesh is called $\tilde{\mathcal{T}}_h$, with vertices $\tilde{\mathcal{V}}_h^1$ (see Figure 3). On $\tilde{\mathcal{T}}_h$, the reconstruction $\tilde{\phi}_h \in V_h^1$ is then characterized by

$$\forall a \in \tilde{\mathcal{V}}_h^1, \quad \tilde{\phi}_h(a) = \begin{cases} \frac{1}{|\mathcal{E}_a|} \sum_{E \in \mathcal{E}_a} \ell_{h|E}(a) & \text{if } a \in \text{int}(\Gamma), \\ \phi_{h,\text{disc}}(a) & \text{otherwise.} \end{cases} \quad (6.4)$$

This reconstruction actually belongs to V because, on the one hand, it is continuous at the interface by definition of the degrees of freedom there (first line of (6.4)) and, on the other hand, it is continuous for all interior facets $F \in \mathcal{F}_h^\Omega \setminus \Gamma$, since we ensure by (6.4) that $(\tilde{\phi}_h)|_F = (\phi_{h,\text{disc}})|_{\Omega_F}$, where Ω_F is the subdomain where F is included. For any element $K \in \mathcal{T}_h$ that does not intersect with the interface, we infer by (6.4) that $(\tilde{\phi}_h)|_K = \phi_{h,\text{disc}}$.

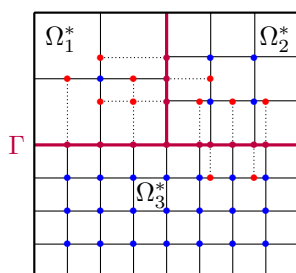


Figure 3: Reconstruction: the set of nodes $\tilde{\mathcal{V}}_h^1$, with newly created red nodes.

Remark 6.2. *In a three-dimensional domain, a reconstruction algorithm can also be derived using the same two-step process. Similar techniques can be applied to simplicial meshes by splitting simplices and forcing the \mathbb{P}^k behaviour on opposite facets.*

6.2 *A posteriori* error estimates

We now detail the derivation of *a posteriori* estimates. The definition of $d_S(\zeta, \xi)$ is extended to piecewise smooth fields on \mathcal{T}_h by replacing \int_{Ω} by $\sum_{i^*=1}^{N^*} \int_{\Omega_{i^*}}$.

Given $K \in \mathcal{T}_h$, we also define π_0^K the $L^2(K)$ -orthogonal projection on the space $L_h^0(K)$, and

$$\begin{aligned} \mathbb{D}_K^{max} &= \sup_{\mathbf{q} \in \mathbf{L}^2(K) \setminus \{0\}} \frac{(\mathbb{D} \mathbf{q}, \mathbf{q})_{0,K}}{\|\mathbf{q}\|_{0,K}^2}, & \mathbb{D}_K^{min} &= \inf_{\mathbf{q} \in \mathbf{L}^2(K) \setminus \{0\}} \frac{(\mathbb{D} \mathbf{q}, \mathbf{q})_{0,K}}{\|\mathbf{q}\|_{0,K}^2}, \\ \Sigma_{a,K}^{max} &= \sup_{\psi \in L^2(K) \setminus \{0\}} \frac{(\Sigma_a \psi, \psi)_{0,K}}{\|\psi\|_{0,K}^2}, & \Sigma_{a,K}^{min} &= \inf_{\psi \in L^2(K) \setminus \{0\}} \frac{(\Sigma_a \psi, \psi)_{0,K}}{\|\psi\|_{0,K}^2}. \end{aligned}$$

In order to state the estimates, at some point we will use the following assumptions, which are identical to those made in the mono-domain case.

Assumption 6.1. *The coefficients \mathbb{D} , Σ_a are piecewise constant on \mathcal{T}_h , and $S_f \in L_h$.*

Assumption 6.2. *The coefficients \mathbb{D}^{-1} , Σ_a are piecewise polynomials on \mathcal{T}_h , and $S_f \in L_h$.*

Finally, we recall that there exists $C_{P,d} > 0$, the so-called Poincaré constant (see eg. Eq. (2.1) in [20]), such that, for all h , for all $K \in \mathcal{T}_h$ and for all $\varphi \in H^1(K)$, it holds that

$$\|\varphi - \pi_0^K \varphi\|_{0,K} \leq C_{P,d} h_K \|\mathbf{grad} \varphi\|_{0,K}. \quad (6.5)$$

Note that $C_{P,d} = \frac{1}{\pi}$ in the case where the considered mesh elements are convex; cf. [18, 2].

We propose two alternatives in the mixed setting (unknown (\mathbf{p}, ϕ)): for the first one we measure the error with respect to the \mathcal{H} norm, while for the second one we use a weighted $\mathbf{H}(\text{div}; \mathcal{T}_h) \times L^2(\Omega)$ norm, with the *broken spaces*

$$\mathbf{H}(\text{div}; \mathcal{T}_h) = \{\mathbf{q} \in \mathbf{L}^2(\Omega) \mid \mathbf{q} \in \mathbf{H}(\text{div}; K), \forall K \in \mathcal{T}_h\}.$$

Both approaches are respectively developed in Sections 6.2.1 and 6.2.2.

6.2.1 Estimates in \mathcal{H} norm

In this section, we use the broken norm associated to the bilinear form d_S , ie.

$$\|\xi\|_{\mathcal{T}_h}^2 = \sum_{K \in \mathcal{T}_h} \|\xi\|_K^2, \text{ where } \|\xi\|_K^2 = \|\mathbb{D}^{-1/2} \mathbf{q}\|_{0,K}^2 + \|\Sigma_a^{1/2} \psi\|_{0,K}^2. \quad (6.6)$$

We note that, according to assumption (3.2) on \mathbb{D} and Σ_a , $\|\cdot\|_{\mathcal{T}_h}$ and $\|\cdot\|_{\mathcal{H}}$ define equivalent norms on \mathcal{H} .

Theorem 6.1. *We suppose that Assumption 5.1 holds. Let $\tilde{\zeta}_h = (\mathbf{p}_h, \tilde{\phi}_h)$ be a reconstruction such that*

$$\forall K \in \mathcal{T}_h, \quad (\Sigma_a \tilde{\phi}_h, 1)_{0,K} = (\Sigma_a \phi_h, 1)_{0,K}. \quad (6.7)$$

For any $K \in \mathcal{T}_h$, we define the residual estimator

$$\bar{\eta}_{r,K} = \bar{m}_K \eta_{r,K}, \quad (6.8)$$

where

$$\eta_{r,K} = \|\Sigma_a^{-1/2} (S_f - \text{div } \mathbf{p}_h - \Sigma_a \tilde{\phi}_h)\|_{0,K} \text{ and } \bar{m}_K = \min \left\{ 1, \frac{C_{P,d} h_K (\Sigma_{a,K}^{max})^{1/2}}{(\mathbb{D}_K^{min})^{1/2}} \right\}, \quad (6.9)$$

and the flux estimator

$$\eta_{f,K} = \|\mathbb{D}^{1/2} (\mathbb{D}^{-1} \mathbf{p}_h + \mathbf{grad } \tilde{\phi}_h)\|_{0,K}. \quad (6.10)$$

One has the reliability estimate

$$\|\|\zeta - \tilde{\zeta}_h\|\|_{\mathcal{T}_h} \leq \left(\sum_{K \in \mathcal{T}_h} \bar{\eta}_{r,K}^2 \right)^{1/2} + \left(\sum_{K \in \mathcal{T}_h} \eta_{f,K}^2 \right)^{1/2}. \quad (6.11)$$

Proof. One can reproduce step-by-step the proof of Theorem 5.4 in [6]. As a matter of fact, it holds that $\tilde{\phi}_h \in V$ and $\mathbf{p}_h \in \mathbf{H}(\text{div}, \Omega)$, thanks to Assumption 5.1 for the latter. This is exactly the required regularity of the reconstruction in the mono-domain case: $\tilde{\zeta}_h \in \mathbf{H}(\text{div}, \Omega) \times V$. \square

This approach may also be applied to the *primal* energy norm. In order to state the following theorem, we define the broken norm

$$\|\|\psi\|\|_{p,\mathcal{T}_h}^2 = \sum_{K \in \mathcal{T}_h} \|\|\psi\|\|_{p,K}^2, \text{ where } \|\|\psi\|\|_{p,K}^2 = \|\mathbb{D}^{1/2} \mathbf{grad } \psi\|_{0,K}^2 + \|\Sigma_a^{1/2} \psi\|_{0,K}^2. \quad (6.12)$$

The equivalent of [6, Theorem 5.4] applies by the same arguments.

Theorem 6.2. *Under the assumptions of Theorem 6.1, one has the reliability estimate*

$$\|\|\phi - \tilde{\phi}_h\|\|_{p,\mathcal{T}_h} \leq \left(\sum_{K \in \mathcal{T}_h} (\bar{\eta}_{r,K} + \eta_{f,K})^2 \right)^{1/2}. \quad (6.13)$$

Theorem 6.3 (local efficiency of the *a posteriori* error estimators). *Let Assumption 6.2 be fulfilled. We suppose that Assumption 5.1 holds. Let $\tilde{\zeta}_h = (\mathbf{p}_h, \tilde{\phi}_h) \in \mathbf{H}(\text{div}, \Omega) \times V$ be a reconstruction. For $K \in \mathcal{T}_h$, let $\bar{\eta}_{r,K}$ and $\eta_{f,K}$ be the residual and flux estimators respectively given by (6.8), and (6.10). In*

addition, we suppose that $\tilde{\phi}_h$ is a piecewise polynomial on \mathcal{T}_h . The following estimates hold true

$$\bar{\eta}_{r,K} \leq \left(\frac{\Sigma_{a,K}^{max}}{\Sigma_{a,K}^{min}} \right)^{1/2} \left(c \frac{\mathbb{D}_K^{max}}{\mathbb{D}_K^{min}} + \mathbf{C} \right)^{1/2} \|\zeta - \tilde{\zeta}_h\|_K \quad (6.14)$$

$$\eta_{f,K} \leq \|\zeta - \tilde{\zeta}_h\|_K + \|\phi - \tilde{\phi}_h\|_{p,K}, \quad (6.15)$$

where c and \mathbf{C} are constants which depend only on the polynomial degree of S_f , Σ_a and $\tilde{\phi}_h$, d , and on the shape-regularity parameter κ_K . If moreover there exists a constant $\kappa > 0$, such that $\min_{K \in \mathcal{T}_h} \kappa_K \geq \kappa$, for all $h > 0$, then the constants c and \mathbf{C} do not depend on κ_K (but on κ).

Proof. The proof is similar to the proof of [6, Theorem 5.5]. \square

As in the mono-domain case, the results of this section extend with the same arguments to the situation where $\Sigma_a \geq 0$ may vanish. Under the assumptions of Theorem 6.1, one has the reliability estimates (6.11) and (6.13) where the residual estimator is now defined as $\bar{\eta}_{r,K} = \eta_{r,K} \bar{m}_K$ with

$$\eta_{r,K} = \begin{cases} (6.9) & \text{if } \inf_K \Sigma_a > 0, \\ \|S_f - \text{div } \mathbf{p}_h - \Sigma_a \tilde{\phi}_h\|_{0,K} & \text{otherwise,} \end{cases} \quad (6.16)$$

and

$$\bar{m}_K = \begin{cases} (6.9) & \text{if } \inf_K \Sigma_a > 0, \\ \frac{C_{P,d} h_K}{(\mathbb{D}_K^{min})^{1/2}} & \text{otherwise.} \end{cases}$$

Under the assumptions of Theorem 6.3, one has the efficiency estimate⁵

$$\bar{\eta}_{r,K} \leq \begin{cases} \left(\frac{\Sigma_{a,K}^{max}}{\Sigma_{a,K}^{min}} \right)^{1/2} \left(c \frac{\mathbb{D}_K^{max}}{\mathbb{D}_K^{min}} + \mathbf{C} \right)^{1/2} \|\zeta - \tilde{\zeta}_h\|_K & \text{if } \inf_K \Sigma_a > 0, \\ \left(c \frac{\mathbb{D}_K^{max}}{\mathbb{D}_K^{min}} + c \frac{\Sigma_{a,K}^{max} h_K^2}{\mathbb{D}_K^{min}} \right)^{1/2} \|\zeta - \tilde{\zeta}_h\|_K & \text{otherwise.} \end{cases}$$

6.2.2 Estimates in strengthened norm

We define the norm $\|\cdot\|_S$ on \mathcal{X} where, for all $\zeta \in \mathcal{X}$,

$$\begin{aligned} \|\zeta\|_S^2 &= d_S(\zeta, \zeta) + \sum_{K \in \mathcal{T}_h} h_K^2 (\mathbb{D}_K^{min})^{-1} \|\text{div } \mathbf{p}\|_{0,K}^2 \\ &= (\mathbb{D}^{-1} \mathbf{p}, \mathbf{p})_{0,\Omega} + (\Sigma_a \phi, \phi)_{0,\Omega} + \sum_{K \in \mathcal{T}_h} h_K^2 (\mathbb{D}_K^{min})^{-1} \|\text{div } \mathbf{p}\|_{0,K}^2. \end{aligned}$$

⁵When $\inf_K \Sigma_a = 0$, there is a h_K^2 factor in the upper bound. One still achieves efficiency, since it holds $h_K \leq \text{diam}(\Omega)$ for all h and all $K \in \mathcal{T}_h$.

Previously, we have seen that, on any given element K , the local efficiency results are purely local (cf. Theorem 6.3), i.e. they involve only quantities defined on the same K . For the strengthened norm, one needs to add quantities defined on the neighboring elements. For $K \in \mathcal{T}_h$, we introduce $N(K) = \{K' \in \mathcal{T}_h \mid \dim_H(\partial K' \cap \partial K) = d - 1\}$, where \dim_H is the Hausdorff dimension, $N^*(K) = N(K) \cap \overline{\Omega_K^*}$ where Ω_K^* is the subdomain which includes K and

$$\mathcal{X}_K = \{\zeta = (\mathbf{p}, \phi) \in \mathbf{PH}(\text{div}, \Omega) \times L^2(\Omega) \mid \text{Supp}(\phi) \subset K, \text{Supp}(\mathbf{p}) \subset N^*(K)\}.$$

Indeed, since \mathbf{p} is in $\mathbf{PH}(\text{div}, \Omega)$, only the elements K' of $N(K)$ that belong to $\overline{\Omega_K^*}$ have to be considered above. In this sense, the definition is slightly different from the one given in the mono-domain case: $N(K)$ is now replaced by $N^*(K)$. Then one can define the following \mathcal{X}_K -local norm, for all $\zeta \in \mathcal{X}$,

$$|\zeta|_{+,K} = \sup_{\xi \in \mathcal{X}_K, \|\xi\|_s \leq 1} d(\zeta, \xi). \quad (6.17)$$

Lemma 6.1. *We suppose that Assumption 5.1 holds. Let $\tilde{\zeta}_h = (\mathbf{p}_h, \tilde{\phi}_h) \in \mathbf{H}(\text{div}, \Omega) \times V$ be a reconstruction. We have for all $\xi = (\mathbf{q}, \psi) \in \mathcal{X}$,*

$$d(\zeta - \tilde{\zeta}_h, \xi) = (S_f - \text{div } \mathbf{p}_h - \Sigma_a \tilde{\phi}_h, \psi)_{0,\Omega} - (\mathbb{D}^{-1} \mathbf{p}_h + \mathbf{grad } \tilde{\phi}_h, \mathbf{q})_{0,\Omega}. \quad (6.18)$$

Proof. According to (4.5), we have

$$d(\zeta - \tilde{\zeta}_h, \xi) = (S_f - \text{div } \mathbf{p}_h - \Sigma_a \tilde{\phi}_h, \psi)_{0,\Omega} - (\mathbb{D}^{-1} \mathbf{p}_h, \mathbf{q})_{0,\Omega} + (\tilde{\phi}_h, \text{div } \mathbf{q})_{0,\Omega}.$$

Owing to the fact that $\tilde{\phi}_h$ is in V , we can integrate by part the last integral:

$$d(\zeta - \tilde{\zeta}_h, \xi) = (S_f - \text{div } \mathbf{p}_h - \Sigma_a \tilde{\phi}_h, \psi)_{0,\Omega} - (\mathbb{D}^{-1} \mathbf{p}_h, \mathbf{q})_{0,\Omega} - (\mathbf{grad } \tilde{\phi}_h, \mathbf{q})_{0,\Omega}.$$

This concludes the proof. \square

Theorem 6.4. *We suppose that Assumption 5.1 holds. Let $\tilde{\zeta}_h = (\mathbf{p}_h, \tilde{\phi}_h) \in \mathbf{H}(\text{div}, \Omega) \times V$ be a reconstruction. For any $K \in \mathcal{T}_h$, we define the residual estimator $\eta_{r,K}$ as in (6.9), the flux estimator $\eta_{f,K}$ as in (6.10). One has the reliability estimate*

$$|\zeta - \tilde{\zeta}_h|_{+,K} \leq \left(\eta_{r,K}^2 + \sum_{K' \in N^*(K)} \eta_{f,K'}^2 \right)^{1/2}. \quad (6.19)$$

Proof. According to Lemma 6.1, we have for all $\xi = (\mathbf{q}, \psi) \in \mathcal{X}$

$$d(\zeta - \tilde{\zeta}_h, \xi) = (S_f - \text{div } \mathbf{p}_h - \Sigma_a \tilde{\phi}_h, \psi)_{0,\Omega} - (\mathbb{D}^{-1} \mathbf{p}_h + \mathbf{grad } \tilde{\phi}_h, \mathbf{q})_{0,\Omega}. \quad (6.20)$$

Let $K \in \mathcal{T}_h$ and ξ be such that $\text{Supp}(\psi) \subset K$, $\text{Supp}(\mathbf{q}) \subset N^*(K)$. Applying Cauchy-Schwarz inequalities successively in $L^2(K)$, $L^2(K')$ for $K' \in N^*(K)$,

and then in $\mathbb{R}^{1+\text{card}(N^*(K))}$, we get

$$\begin{aligned} & d(\zeta - \tilde{\zeta}_h, \xi) \\ & \leq \eta_{r,K} \|\Sigma_a^{1/2} \psi\|_{0,K} + \sum_{K' \in N^*(K)} \eta_{f,K'} \|\mathbb{D}^{-1/2} \mathbf{q}\|_{0,K'} \\ & \leq \left(\eta_{r,K}^2 + \sum_{K' \in N^*(K)} \eta_{f,K'}^2 \right)^{1/2} \left(\|\Sigma_a^{1/2} \psi\|_{0,K}^2 + \sum_{K' \in N^*(K)} \|\mathbb{D}^{-1/2} \mathbf{q}\|_{0,K'}^2 \right)^{1/2}. \end{aligned}$$

We infer (6.19) from the definition of the $|\cdot|_{+,K}$ norm (6.17). \square

Theorem 6.5 (local efficiency of the *a posteriori* error estimators). *Let Assumption 6.2 be fulfilled. We suppose that Assumption 5.1 holds. Let $\tilde{\zeta}_h = (\mathbf{p}_h, \tilde{\phi}_h) \in \mathbf{H}(\text{div}, \Omega) \times V$ be a reconstruction. For $K \in \mathcal{T}_h$, let $\eta_{r,K}$ and $\eta_{f,K}$ be the residual and flux estimators respectively given by (6.9), and (6.10). In addition, we suppose that $\tilde{\phi}_h$ is piecewise polynomial on \mathcal{T}_h . The following estimates hold true*

$$\eta_{r,K} \leq \mathbf{c} \left(\frac{\Sigma_{a,K}^{\max}}{\Sigma_{a,K}^{\min}} \right)^{1/2} |\zeta - \tilde{\zeta}_h|_{+,K}, \quad (6.21)$$

$$\eta_{f,K} \leq \mathbf{C} \left(\frac{\mathbb{D}_K^{\max}}{\mathbb{D}_K^{\min}} \right)^{1/2} |\zeta - \tilde{\zeta}_h|_{+,K}, \quad (6.22)$$

where \mathbf{c} and \mathbf{C} are constants which depend only on the polynomial degree of S_f , \mathbb{D} , Σ_a and $\tilde{\phi}_h$, d , and the shape-regularity parameter κ_K . If moreover there exists a constant $\kappa > 0$, such that $\min_{K \in \mathcal{T}_h} \kappa_K \geq \kappa$, for all $h > 0$, then the constants \mathbf{c} and \mathbf{C} do not depend on κ_K (but on κ).

Proof. The proof is completely similar to the proof of [6, Theorem 5.7]. \square

Similarly to the comments at the end of Section 6.2.1, the results of this section extend with the same arguments to the situation where $\Sigma_a \geq 0$ may vanish if one slightly modifies the definition of the norms by

$$\begin{aligned} \|\zeta\|_{S,\star}^2 &= (\mathbb{D}^{-1} \mathbf{p}, \mathbf{p})_{0,\Omega} + (\Sigma_\star \phi, \phi)_{0,\Omega} + \sum_{K \in \mathcal{T}_h} h_K^2 (\mathbb{D}_K^{\min})^{-1} \|\text{div } \mathbf{p}\|_{0,K}^2, \\ |\zeta|_{+,\star,K} &= \sup_{\xi \in \mathcal{X}_K, \|\xi\|_{S,\star} \leq 1} d(\zeta, \xi), \end{aligned}$$

where Σ_\star is defined for all $K \in \mathcal{T}_h$ by

$$\Sigma_\star|_K = \begin{cases} \Sigma_a & \text{if } \inf_K \Sigma_a > 0, \\ \sup_K \Sigma_a & \text{if } \inf_K \Sigma_a = 0 \text{ and } \sup_K \Sigma_a > 0, \\ 1 & \text{otherwise.} \end{cases}$$

Let us define for all $K \in \mathcal{T}_h$,

$$\Sigma_{\star,K}^{max} = \sup_{\psi \in L^2(K) \setminus \{0\}} \frac{(\Sigma_{\star} \psi, \psi)_{0,K}}{\|\psi\|_{0,K}^2}, \quad \Sigma_{\star,K}^{min} = \inf_{\psi \in L^2(K) \setminus \{0\}} \frac{(\Sigma_{\star} \psi, \psi)_{0,K}}{\|\psi\|_{0,K}^2}.$$

Under the assumptions of Theorem 6.4, one has the reliability estimate

$$|\zeta - \tilde{\zeta}_h|_{+,K} \leq \left(\eta_{r,\star,K}^2 + \sum_{K' \in N^*(K)} \eta_{f,K'}^2 \right)^{1/2},$$

where the residual estimator becomes $\bar{\eta}_{r,\star,K} = \eta_{r,\star,K} \bar{m}_{\star,K}$ with

$$\eta_{r,\star,K} = \|\Sigma_{\star}^{-1/2} (S_f - \operatorname{div} \mathbf{p}_h - \Sigma_a \tilde{\phi}_h)\|_{0,K},$$

$$\bar{m}_{\star,K} = \min \left\{ 1, \frac{C_{P,d} h_K (\Sigma_{\star,K}^{max})^{1/2}}{(\mathbb{D}_K^{min})^{1/2}} \right\}.$$

Under the assumptions of Theorem 6.5, one has the efficiency estimates

$$\eta_{r,\star,K} \leq \mathbf{c} \left(\frac{\Sigma_{\star,K}^{max}}{\Sigma_{\star,K}^{min}} \right)^{1/2} |\zeta - \tilde{\zeta}_h|_{+,\star,K},$$

$$\eta_{f,K} \leq \mathbf{c} \left(\frac{\mathbb{D}_K^{max}}{\mathbb{D}_K^{min}} \right)^{1/2} |\zeta - \tilde{\zeta}_h|_{+,\star,K}.$$

7 Numerical results

In this section, we illustrate numerically the use of the a posteriori estimators devised in the previous section. To this aim, we present an example of Adaptive Mesh Refinement (AMR) in the same framework as [6, Section 6]. Next, we are interested in the case of heterogeneous coefficients which may induce some singularities in the solution of Problem (5.3), that is a loss of regularity of the solution due to the discontinuities of the coefficients.

Section 7.1 defines the adaptive mesh refinement process. Then, the test case is introduced in Section 7.2. Numerical results are shown in Section 7.3.

7.1 Adaptive mesh refinement

In this section, we aim to illustrate an AMR strategy on Problem (5.3). This iterative process is divided into four modules as presented in Figure 4.

The module **SOLVE** amounts to solving the source problem (5.3). In module **ESTIMATE**, the local error indicator η_K is computed on each element $K \in \mathcal{T}_h$ from a posteriori error estimates (cf. Section 6.2). The stopping criterion is defined as $\max_{K \in \mathcal{T}_h} \eta_K \leq \varepsilon_{\text{AMR}}$ for a user-defined $\varepsilon_{\text{AMR}} > 0$.

The purpose of the module **MARK** is to select a set of elements with large error

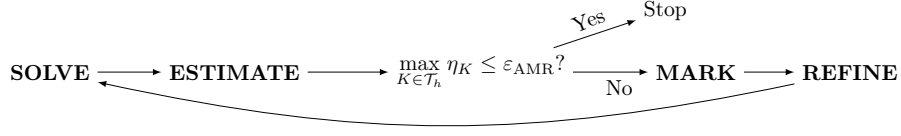


Figure 4: Description of the AMR process.

to be refined in each mesh \mathcal{T}_{h,i^*} , $1 \leq i^* \leq N^*$. The marking strategy consists in finding for all $1 \leq i^* \leq N^*$ an optimal set of cells S_{i^*} such that one has

$$\eta(S_{i^*}) \leq \theta_{i^*} \eta(\mathcal{T}_{h,i^*}), \quad \text{where} \quad \eta(S) := \left(\sum_{K \in S} \eta_K^2 \right)^{1/2},$$

and $\theta_{i^*} > 0$ is a user-defined parameter. According to [6, Section 6], an efficient strategy which preserves the Cartesian structure of the mesh is the *direction* marker strategy. One selects for each direction \mathbf{e}_x , $x = 1, \dots, d$, the smallest set of lines $L_{x,i^*} \subset \mathcal{T}_{h,i^*}$ such that $\eta(L_{x,i^*}) \geq \theta_{i^*} \eta(\mathcal{T}_{h,i^*})$. The resulting selected set is $\cup_{1 \leq i^* \leq N^*, x=1, \dots, d} L_{x,i^*}$.

Finally, the module **REFINE** refines, for all $1 \leq i^* \leq N^*$, the mesh \mathcal{T}_{h,i^*} if the stopping criterion is not reached locally i.e. $\max_{K \in \mathcal{T}_{h,i^*}} \eta_K > \varepsilon_{\text{AMR}}$.

In Section 7.3, we apply the *direction* marker strategy and use a relative stopping criterion defined by $\varepsilon_{\text{AMR}} = \varepsilon_{\text{AMR, rel}} \|\phi_h\|_{L^2(\Omega)}$, where $\varepsilon_{\text{AMR, rel}} > 0$ and

$$\eta_K := \left(\eta_{r,K}^2 + \sum_{K' \in N^*(K)} \eta_{f,K'}^2 \right)^{1/2},$$

where we apply the reconstruction operator defined in Section 6.1.2.

7.2 Settings of the test case

We choose a benchmark dedicated to shielding applications [10, Section 5.2]. The geometry is a 3×3 grid composed of squares of size 10cm, and we set $\Omega = (0, 30)^2$. In the test case, there are two materials. The first material is located in the center of the grid $(10, 20)^2$, and we set $\Sigma_a = 0.5$, $D = 1/3$, $S_f = 1$. In the second material, we fix $\Sigma_a = 1.9$, $D = 1/6$, $S_f = 0$. Figure 5 displays the so-called reference solution.

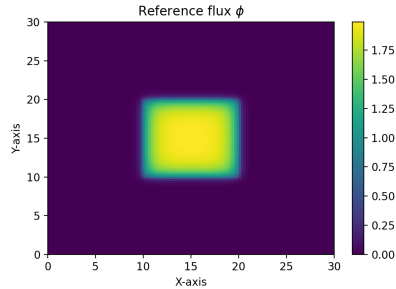


Figure 5: Reference solution

The initial mesh is a uniform Cartesian mesh of size 2.5cm and the discretization is performed with RTN_0 and \mathbb{Q}^0 finite elements. In the DD+ L^2 jumps method, we set M_h as in (5.6). Figure 6 shows the three tested domain decomposition configurations:

- Case 1 : Cartesian 2×1 grid ($N^* = 2$);
- Case 2 : non-Cartesian grid ($N^* = 3$);
- Case 3 : Cartesian 3×3 grid.

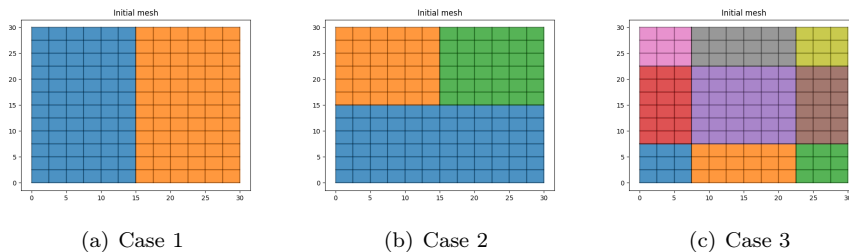


Figure 6: Different configurations of domain decomposition.

We compare three different refinement strategies: uniform refinement, AMR with a monodomain discretization [6] and AMR with DD+ L^2 jumps method.

The stopping criterion is set to $\varepsilon_{\text{AMR, rel}} = 0.01$.

We apply the AMR process defined above for the DD+ L^2 jumps method. The ESTIMATE module is based on the estimators of the strengthened norm defined in (6.19) and the averaging method described in Section 6.1.2. In the REFINE module, we fix $\theta_{i^*} = 0.5$ for all $1 \leq i^* \leq N^*$, except in the subdomain of Case 3 grid located at $(7.5, 22.5)^2$ where we set $\theta = 0.3$.

Correspondingly, we apply the AMR process for the monodomain formulation [6, Section 6.1]. The ESTIMATE module is based on the estimators of the strengthened norm [6, Theorem 5.6] and the averaging method described in [6, Section 5.1.1]. In the REFINE module, we fix $\theta = 0.5$.

7.3 Numerical illustration

Table 1 shows that all AMR processes are reaching the stopping criterion with significantly less mesh elements than uniform refinement. We also observe that

Iter	Uniform		Monodomain		DD+ L^2 -jumps Case 1		DD+ L^2 -jumps Case 2		DD+ L^2 -jumps Case 3	
	$ \mathcal{T}_h $	$\max_{K \in \mathcal{T}_h} \eta_K$	$ \mathcal{T}_h $	$\max_{K \in \mathcal{T}_h} \eta_K$	$ \mathcal{T}_h $	$\max_{K \in \mathcal{T}_h} \eta_K$	$ \mathcal{T}_h $	$\max_{K \in \mathcal{T}_h} \eta_K$	$ \mathcal{T}_h $	$\max_{K \in \mathcal{T}_h} \eta_K$
0	144	1.970	144	1.970	144	1.970	144	1.970	144	1.782
1	576	0.962	256	1.376	256	1.755	256	1.526	244	1.721
2	2304	0.422	441	0.958	462	0.946	473	0.909	396	1.290
3	9216	0.170	784	0.596	810	0.504	855	0.463	465	0.828
4	10000	0.161	1296	0.290	1360	0.272	1480	0.269	552	0.595
5	-	-	2209	0.208	2214	0.196	1934	0.196	696	0.341
6	-	-	3844	0.135	3952	0.124	2814	0.124	921	0.149

Table 1: Comparison between meshes and estimators for the different configurations.

the final number of mesh elements is similar between the monodomain discretization and the DD+ L^2 jumps method in Cases 1 and 2. On the other hand, one of the well-known advantages of the domain decomposition approach is to allow for parallelization (not implemented here).

Comparing the domain decomposition configurations, the AMR process in Case 3 yields a coarser mesh than the other AMR processes by a multiplicative factor greater than 3 in terms of the total number of mesh elements.

Figure 7 shows the final refined meshes.

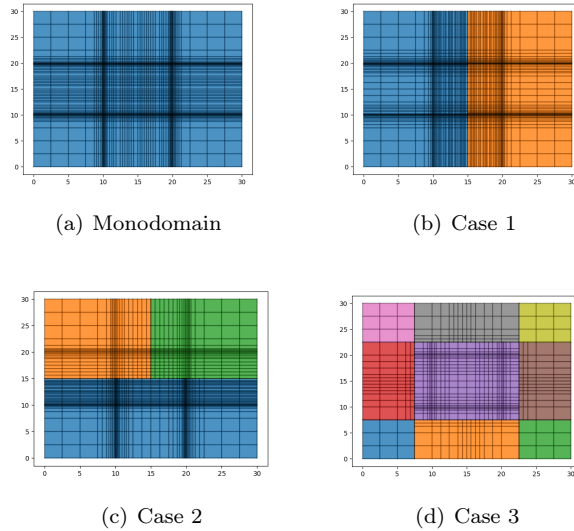


Figure 7: Final meshes for the different configurations.

Finally, Table 2 details the convergence of the AMR process in Case 3 on each subdomain $\Omega_{i^*}^*$, $1 \leq i^* \leq 9$. We observe that the convergence of the AMR process focuses on the subdomain located at $(7.5, 22.5)^2$, which is precisely the subdomain that encompasses the interface between the two materials.

Iter	$ \mathcal{T}_k $	DD+ L^2 -jumps - Case 3									
		$\max_{K \in \mathcal{T}_{h,1}} \eta_K$	$\max_{K \in \mathcal{T}_{h,2}} \eta_K$	$\max_{K \in \mathcal{T}_{h,3}} \eta_K$	$\max_{K \in \mathcal{T}_{h,4}} \eta_K$	$\max_{K \in \mathcal{T}_{h,5}} \eta_K$	$\max_{K \in \mathcal{T}_{h,6}} \eta_K$	$\max_{K \in \mathcal{T}_{h,7}} \eta_K$	$\max_{K \in \mathcal{T}_{h,8}} \eta_K$	$\max_{K \in \mathcal{T}_{h,9}} \eta_K$	
0	144	0.003	0.544	0.003	0.544	1.782	0.544	0.003	0.544	0.003	
1	244	-	0.247	-	0.247	1.721	0.247	-	0.247	-	
2	396	-	0.012	-	0.012	1.290	0.012	-	0.012	-	
3	465	-	-	-	-	0.828	-	-	-	-	
4	552	-	-	-	-	0.595	-	-	-	-	
5	696	-	-	-	-	0.341	-	-	-	-	
6	921	-	-	-	-	0.149	-	-	-	-	

Table 2: Case 3 : AMR with the DD+ L^2 -jumps. Starting from the bottom left, the subdomains are indexed from left to right, then from bottom to top.

8 Conclusion

In this manuscript, we extend *a posteriori* estimates associated to different norms for the DD+ L^2 jumps method for the neutron diffusion equation. Remarkably, no reconstruction of the Lagrange multiplier is needed to achieve the optimal *a posteriori* estimates. In a companion paper, we will study a more general model, widely used for nuclear core simulations, the multigroup diffusion problem, for which we will also provide *a posteriori* estimators that can be proven to be reliable and locally efficient.

References

- [1] T. Arbogast and Z. Chen. On the implementation of mixed methods as nonconforming methods for second-order elliptic problems. *Math. Comp.*, 64(211):943–972, 1995.
- [2] M. Bebendorf. A note on the poincaré inequality for convex domains. *Zeitschrift für Analysis und ihre Anwendungen*, 22(4):751–756, 2003.
- [3] D. Boffi, F. Brezzi, and M. Fortin. *Mixed and hybrid finite element methods and applications*. Springer-Verlag, 2013.
- [4] C. Carstensen. A posteriori error estimate for the mixed finite element method. *Math. Comp.*, 66(218):465–476, 1997.
- [5] P.G. Ciarlet. *The finite element method for elliptic problems*, volume 40 of *Classics in Applied Mathematics*. SIAM, 2002.
- [6] P. Ciarlet, Jr., M.H. Do, and F. Madiot. A posteriori error estimates for mixed finite element discretizations of the neutron diffusion equations. *ESAIM: Math. Modell. Numer. Anal.*, 57(1):1–27, 2023.

- [7] P. Ciarlet, Jr., L. Giret, E. Jamelot, and F. D. Kpadonou. Numerical analysis of the mixed finite element method for the neutron diffusion eigenproblem with heterogeneous coefficients. *ESAIM: Math. Modell. Numer. Anal.*, 52:2003–2035, 2018.
- [8] P. Ciarlet, Jr., E. Jamelot, and F. D. Kpadonou. Domain decomposition methods for the diffusion equation with low-regularity solution. *Comput. Math. Applic.*, 74:2369–2384, 2017.
- [9] J. J. Duderstadt and L. J. Hamilton. *Nuclear reactor analysis*. John Wiley & Sons, Inc., 1976.
- [10] J.I. Duo, Y.Y. Azmy, and L.T. Zikatanov. A posteriori error estimator and amr for discrete ordinates nodal transport methods. *Annals of Nuclear Energy*, 36(3):268–273, 2009. PHYSOR 2008.
- [11] A. Ern and J.-L. Guermond. *Finite elements II*. Springer-Verlag, 2021.
- [12] E. Jamelot, A.-M. Baudron, and J.-J. Lautard. Domain decomposition for the SP_N solver MINOS. *Transport Theory and Statistical Physics*, 41(7):495–512, 2012.
- [13] E. Jamelot and P. Ciarlet, Jr. Fast non-overlapping Schwarz domain decomposition methods for solving the neutron diffusion equation. *J. Comput. Phys.*, 241:445–463, 2013.
- [14] M. G. Larson and A. Målqvist. A posteriori error estimates for mixed finite element approximations of elliptic problems. *Numer. Math.*, 108(3):487–500, 2008.
- [15] C. Lovadina and R. Stenberg. Energy norm a posteriori error estimates for mixed finite element methods. *Math. Comp.*, 75(256):1659–1674, 2006.
- [16] J.-C. Nédélec. Mixed finite elements in \mathbb{R}^3 . *Numer. Math.*, 35(3):315–341, 1980.
- [17] P. Oswald. On a BPX-preconditioner for P1 elements. *Computing*, 51(2):125–133, 1993.
- [18] L. E. Payne and H. F. Weinberger. An optimal poincaré inequality for convex domains. *Archive for Rational Mechanics and Analysis*, 5(1):286–292, January 1960.
- [19] P.-A. Raviart and J.-M. Thomas. A mixed finite element method for second order elliptic problems. In *Mathematical aspects of finite element methods*, volume 606 of *Lecture Notes in Mathematics*, pages 292–315. Springer, 1977.
- [20] M. Vohralík. A posteriori error estimates for lowest-order mixed finite element discretizations of convection-diffusion-reaction equations. *SIAM J. Numer. Anal.*, 45(4):1570–1599, 2007.

- [21] M. Vohralík. Unified primal formulation-based a priori and a posteriori error analysis of mixed finite element methods. *Math. Comp.*, 79(272):2001–2032, 2010.
- [22] M. F. Wheeler and I. Yotov. A posteriori error estimates for the mortar mixed finite element method. *SIAM J. Numer. Anal.*, 43(3):1021–1042, 2005.
- [23] B. Wohlmuth and R. Hoppe. A comparison of a posteriori error estimators for mixed finite element discretizations by Raviart-Thomas elements. *Math. Comp.*, 68(228):1347–1378, 1999.